CONF-791058--36

CALCULATED PARTICLE PRODUCTION SPECTRA AND MULTIPLICITIES FROM NUCLEON-FISSILE ELEMENT COLLISIONS AT MEDIUM ENERGIES

F. S. Alsmiller, R. G. Alsmiller, Jr., T. A. Gabriel, R. A. Lillie, J. Barish
Oak Ridge National Laboratory
Oak Ridge, Tennessee 37830, USA

A fission channel has been added to the intranuclear-cascade-evaporation model of nuclear reactions so that this model may be used to obtain the differential particle production data that are needed to study the transport of medium-energy nucleons and pions through matter. The earlier work of Hahn and Bertini on the incorporation of fission-evaporation competition into the intranuclear-cascade-evaporation model has been retained and the statistical model of fission has been utilized to predict particle production from the fission process. Approximate empirically derived kinetic energies and deformation energies are used in the statistical model. The calculated residual nuclei distributions are in reasonable agreement with experimental data, but the neutron multiplicities at the higher incident nucleon energies $\gtrsim$ 500 MeV are sensitive to the level density parameter used.

[High Energy Cross Sections, Actinide Fission, Statistical Model, Intranuclear Cascade]

Introduction

For several applications, e.g., studies of the feasibility of converting fertile to fissile material using medium-energy proton beams[1], and in designing facilities to produce an intense source of low-energy neutrons by using medium-energy protons[2], it is necessary to carry out calculations of the transport of medium- and low-energy nucleons and pions through fissionable material. To carry out such transport calculations it is necessary to have available differential particle production data from the collision of nucleons and pions with fissionable nuclei. In this paper a fission channel, that has been added to the intranuclear-cascade-evaporation model of H. W. Bertini[3,4] so that this model can be used to provide this needed differential particle production data, is described and comparisons between calculational results and experimental data are presented.

In a previous paper, H. L. Hahn and H. W. Bertini[5] have shown how the probability of fission may be incorporated into the intranuclear-cascade-evaporation model, but they did not extend their calculations to include particle production following fission. In the present paper, this particle production following fission is included by using a version of the statistical model of fission developed by P. Fong.[6] To a large extent the physical data that occur in the statistical model have been derived from the experimental measurements of D. H. Epperson.[7] Calculations similar to those presented here have previously been given by V. S. Barashenkov and V. D. Toneyev.[8] In the model used here, however, much more reliance is placed on empirically derived constants than in Ref. 8.

Intranuclear-Cascade-Evaporation Model

The intranuclear-cascade-evaporation model of medium-energy nuclear reactions as implemented by Bertini has been described in detail previously[3,4], so only a very simple discussion of those parts of the model that have not been modified will be given here. Basically, the model assumes that nucleon- and pion-nucleus nonelastic collisions may be considered to be a two-step process. In the first step the cascade nucleons and pions are emitted leaving an exicted residual nucleus. In the second step this excited nucleus loses its excitation energy by "evaporating" particles. If the excited residual nucleus has a sufficiently large atomic weight and number, fission will compete with the evaporation process. Hahn and Bertini[5] have considered this competition and have found that reasonably reliable results can be obtained by using an excitation-energy-independent empirically derived formula for the ratio of the neutron width to the fission width in conjunction with the assumption that no fission occurs for elements with atomic number less than 91. After a fission has occurred, two excited residual nuclei remain and further particle emission by evaporation occurs. The work reported here is primarily concerned with estimating the mass, atomic number, and kinetic energy distributions of the nuclei produced from fission and with estimating the kind, number and energy of the particles that are evaporated following fission.

Statistical Model

Let the set (A_f, z_f, m_{of}, E_f) be the nucleon number, proton number, rest mass energy, and excitation energy of the fissioning nucleus. Similarly, let the set $(A_i, z_i, m_{oi}, E_{ir})$ be the corresponding values for the fission fragments where i takes values 1 and 2 corresponding to the light and heavy fragment and r takes values S meaning evaluation at scission time, t_S, and E meaning evaluation at evaporation time, t_E. If

$$m_d = m_{of} - m_{o1} - m_{o2} \; ; \; Q = E_f + m_d \; , \qquad (1)$$

conservation of energy gives[6,9]

$$E_{1E} + E_{2E} = Q - K_E = E_{1S} + E_{2S} + D \; , \qquad (2)$$

where D is the total "deformation" energy at t_S and K_E is the relative kinetic energy at t_E. Also

$$K_E = K_S + C_S \; ; \; C_S = k \, V_S \; , \qquad (3)$$

where K_S is the relative kinetic energy at t_S, C_S is the Coulomb potential energy of the deformed fragments at t_S, and V_S is the Coulomb potential energy of two spherical nuclei in contact.

Conservation of momentum can be carried out relativistically at t_E in the c.m. system. Then

$$\sqrt{p^2+m_{e1}^2} + \sqrt{p^2+m_{e2}^2} = \varepsilon_1 + \varepsilon_2 = m_{ef} \qquad (4)$$

$$m_{ei} = m_{oi} + E_{iE} \qquad i = 1,2 \qquad (5)$$

$$m_{ef} = m_{of} + E_f = K_E + m_{e1} + m_{e2} \; , \qquad (6)$$

and P, the magnitude of the momentum of each fragment, is given by

$$p^2 \simeq 2K_E \, \frac{m_{e1} m_{e2}}{m_{ef}} \qquad (7)$$

DISCLAIMER

The kinetic energies of each fragment are obtained using the value of P from Eq. (7) and isotropy in the c.m. system. The density of kinetic energy states will be needed in the statistical model. The relativistic value for this is proportional to $\omega(K_E)$ where

$$\omega(K_E) = P^2 \frac{dP}{dK_E} = \frac{\varepsilon_1\varepsilon_2 P}{m_{ef}} \simeq \frac{A_1A_2}{A_1+A_2}\sqrt{K_E} \qquad (8)$$

The primary postulate of the statistical theory of Fong[6] is that the yield of fission fragments, $N(A_2,E_f)$, is taken to be proportional to the total density of quantum states at scission time, integrated over all variables. The density of excitation states at t_S is written

$$\tilde{\rho}_{iS} = p_{ri} \exp\left[2\sqrt{a_i E_{ic}}\right] \qquad i = 1,2 \qquad (9)$$

$$E_{ic} = E_{iS} - \Delta_i = E_{iE} - \Delta_i - D_i \qquad (10)$$

= excitation energy above the "characteristic" ground-state level[6],

Δ_i = pairing energy,

p_{ri} = preexponential factor, including an integral over all angular momentum states,

a_i = "level density parameter."

For given deformation energies, D_i, the product $\tilde{\rho}_{1S}\tilde{\rho}_{2S}\,\omega(K_E)$, where $\omega(K_E)$ has been given previously, is proportional to the total density of states. Defining

$$R_m = Q - \Delta_1 - \Delta_2 \ , \qquad (11)$$

$P(D,k)$ = probability of a given D and k,

one can write quite generally, using limits determined by the conservation of energy conditions,

$$N(A_2,E_f) \triangleq \int_{z_L}^{z_H} dz_2 \int_{D_{min}}^{R_m-k_{min}V_s} dD \int_{k_L(D)\geq k_{min}}^{(R_m-D)/V_s} dk \int_{kV_s}^{R_m-D} dK_E \int_0^{R_m-D-K_E} dE_{2c}$$

$$\times\, \tilde{\rho}_{2S}(E_{2c})\tilde{\rho}_{1S}(R_m-D-K_E-E_{2c})\omega(K_E)P(D,k) \ . \qquad (12)$$

The limits z_L, z_H, $k_{min} > 0$, and $D_{min}(z_2) > 0$, are assumed tentatively to be given.

The probability function, $P(D,k)$, and the lower limit, $k_L(D)$, must be found from a theory of deformation energies. For simplicity, we use the two-parameter theory of Fong[10],

$$D_i = \frac{C_i}{2}\beta_i^2 \qquad i = 1,2 \qquad (13)$$

$$D = D_1+D_2 = D_2(1+D_r) \ ; \ D_r = \frac{C_1}{C_2}\beta_{1r} \ ; \beta_{1r} = \frac{\beta_1}{\beta_2} \qquad (14)$$

$$k = C_S/V_S = \frac{(r_1+r_2)_s}{r_{1s}+r_{2s}+\alpha_1\beta_1 r_{1s}+\alpha_2\beta_2 r_{2s}} \ , \qquad (15)$$

where r_{1s} = radius of spherical nucleus, α_1, and α_2 are parameters (or functions of A_2,z_2) to be determined, and the C's are Mottelson's "stiffness coefficients", furnished by Fong[10,11].

One can solve for $\beta_{1r}(D,k)$. The minimum possible value of k, if β_{1r} is to be real, is given by

$$k_L(D) = \left[1+\sqrt{D/D_o}\,\right]^{-1} \ ; \ D_o = \frac{C_2\left[\left(1+\frac{r_{1s}}{r_{2s}}\right)/\alpha_2\right]^2}{2(1+D_{rp})} \qquad (16)$$

$$D_{rp} = \frac{C_2}{C_1}\left(\frac{\alpha_1 r_{1s}}{\alpha_2 r_{2s}}\right) \ ; \ \frac{r_{1s}}{r_{2s}} = \left(\frac{A_1}{A_2}\right)^{1/3} . \qquad (17)$$

Conversely, the minimum possible value of D(k) is

$$D_L(k) = D_o(1/k-1)^2 .$$

Integrations in Eq. (12) are interchanged systematically so as to bring them into the order: K_E, z_2, E_{2c}, D and k. The upper limit of the E_{2c} integration is E_m where

$$E_m = R_m - K_E - D_{low}(K_E,z_2) \geq 0 \ . \qquad (18)$$

$$D_{low}(K_E,z_2) = D_L(K_E/V_s) \ , \ \text{if } \frac{K_E}{V_s} < k_L(D_{min}) = k_c \qquad (19)$$

$$= D_{min}(z_2), \ \text{if } \frac{K_E}{V_s} \geq k_L(D_{min}) = k_c .$$

The K_E and z_2 integration limits can be worked out to satisfy Eq. (18). Gaussian-type integrations, carried out in Fong's[6] manner give

$$N(A,E_f) \ \exp\left[2\sqrt{(a_1+a_2)\bar{E}_m}\right]\sigma_{K_E}\bar{\sigma}_z\bar{\sigma}_{E_{2c}}\,\bar{p}_{r1}\bar{p}_{r2}\bar{I}_{nn} \qquad (20)$$

$$\bar{E}(A_2,E_f) \equiv \bar{E}_m = \bar{R}_m - \bar{K}_E - \bar{D} \ ; \ \bar{D} = D_{low}(\bar{K}_E,\bar{z}_2) \qquad (21)$$

$$\equiv E_f + \overline{\Delta E_c}\,(A_2,E_f) \ . \qquad (22)$$

The overbars indicate evaluation at a "most probable" value of $z_2 = \bar{z}_2$ and at $\bar{K}_E$, the average value of K_E. Both $\bar{K}_E$ and σ_{K_E}, the variance of the K_E distribution, are taken from experiment, for p on U^{235} (see next section); $\bar{\sigma}_z$ is the variance of the z_2 distribution for fixed K_E, evaluated at $\bar{K}_E$; $\bar{\sigma}_{E_{2c}}$ is the average of the variance given by the integral, (approximately integrated by Fong[6]),

$$\sigma_{E_{2c}} = \frac{\exp\left[-2\sqrt{(a_1+a_2)\bar{E}_m}\,\right]}{\bar{p}_{r2}\bar{p}_{r1}} \int_0^{E_m} dE_{2c} \, \frac{\exp\left[2\sqrt{a_2E_{2c}}\,\right]}{\exp\left[-2\sqrt{a_1(E_m-E_{2c})}\,\right]} \times p_{r1}p_{r2} \qquad (23)$$

$$\triangleq \frac{(a_1a_2)^{1/2}}{(a_1+a_2)^{5/4}}\,E_m^{3/4} .$$

The value of $\bar{z}_2$ is found approximately from the condition

$$\frac{d}{dz_2}E_m = 0 \ , \qquad (24)$$

using the Fong-Wing[12] empirical mass formula. Rest mass and pairing energies, taken from Wapstra[13] and Cameron[14] are interpolated to obtain $\bar{R}_m = R_m(A_2,\bar{z}_2)$. For the level density parameters, a_i, we used the formula[15]

$$a_i = \frac{A_i}{B_o}\left[1 + Y_o(A_i-z_i)^2/A_i^2\right] \ , \qquad (25)$$

where B_0 and Y_0 are constants.

In this paper, the factors $\bar{\sigma}_z\ \bar{p}_{r1}\bar{p}_{r2}\bar{I}_{nn}$ were taken to be approximately those used by Fong[6].

The function D_0 in Eq. (16) was evaluated using

$$D_0 = \bar{D}_0 = \bar{D}(\bar{V}_s/\bar{K}_E - 1)^2 \qquad (26)$$

The Monte Carlo procedures to select the needed parameters for a random mass splitting are to sample A_2 from Eq. (20) by rejection techniques; sample K_E and z_2 from truncated Gaussians; sample E_2 from the integrand of Eq. (23) by rejection. Then

$$E_{2E} = E_{2c} + \Delta_2 + D_2\ ;\ D_2 = D_{low}(K_E,z_2)/(1+D_{rp}) \qquad (27)$$
$$E_{1E} = (E_m - E_{2c}) + \Delta_1 + D_2\ D_{rp}\ .$$

Empirical Determination of Deformation Energy, Mean Kinetic Energy, and Variance of the Kinetic Energy

Correlated experimental postevaporation distributions versus A_2 for the residual nuclei yields, $Y(A_2,E_I)$, average total kinetic energy of the fragment pair, and the variance of the kinetic energy for protons of kinetic energy, E_I, ($\leq$ 30 MeV) incident on U^{235} are available from Epperson. In principle, each of these distributions is an integral over E_f of a preevaporation distribution weighted by the probability of fission at E_f. Neglecting any dependence on the prefission values of A_f and z_f, the prefission distributions may be obtained approximately from the postevaporation distribution by using an average emitted evaporation neutron multiplicity $\bar{\nu}$. Thus, taking six values of the incident proton energy, i.e., E_{Ij} for j = 1 to 6, and corresponding intervals in E_f, each with average value E_{fj}, one has

$$Y_j(A_2,E_{Ij}) = \sum_{k=1}^{j} P_f(E_{fk})\Delta E_{fk} N_k(A'_{2k},E_{fk}) \qquad j=1,6$$
$$A'_{2k} = A_2 + \bar{\nu}(E_{fk}) \qquad (28)$$

which may easily be solved for $N_k(A'_{2k},E_{fk})$. The E_{Ij} values used were 7, 10, 15, 20, 25, and 30 MeV and the fission probabilities and neutron multiplicities were computed by using the intranuclear-cascade-evaporation model including the fission channel described in this paper. The N_j's were obtained from Eq. (28) for $E_f \leq E_{f6}$. The same procedure was followed to obtain the functions $\bar{K}_E(A_2,E_{fj})$ and $\sigma_{K_E}(A_2,E_{fj})$.

The next step in the procedure was to fit the yields $N_j(A_2,E_{fj})$ by use of Eq. (20) from the statistical model. In this fitting procedure the quantity $\bar{E}(A_2,E_{fj})$ was determined, and then the quantities $\overline{\Delta E_c}(A_2,E_{fj})$, $\bar{K}_E(A_2,E_{fj})$ and $\sigma_{K_E}(A_2,E_{fj})$ for N_p^{236} form a permanent data set for use in the statistical model code. Interpolation between the values of E_{fj} was used to obtain data at all values less than E_{f6}. When the excitation energy exceeds that corresponding to an incident proton energy of 30 MeV the values of these functions (and the derived average deformation energy) are simply assumed to have the value calculated at E_{f6}.

When the fissioning nucleus is not N_p^{236} a simple scaling procedure is assumed. Thus, if primes are used to indicate values corresponding to N_p^{236},

$$A_2 = \frac{A_f}{236}\,A'_2 \qquad (29)$$

$$\bar{E}(A_2,E_f) = \left[\frac{(a_1+a_2)_{236}}{(a_1+a_2)_{A_f}}\right] E'(A'_2,E_f)\ . \qquad (30)$$

The functions $K_E(A_2,E_f)$ and $\sigma_{K_E}(A_2,E_f)$ are arbitrarily scaled in the same manner as $\bar{E}(A_2,E_f)$. These assumptions modify the distributions just enough to give the correct reflection in A_2 (since the statistical model predicts symmetrically reflected distributions) and to maintain general shapes.

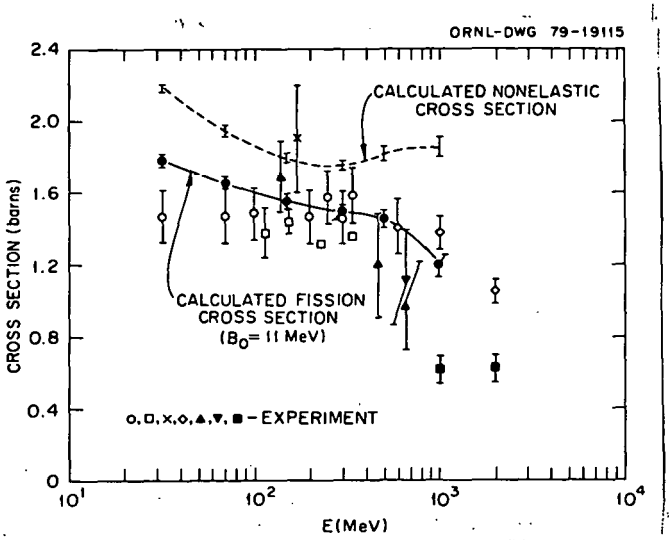

Fig. 1. Nonelastic and fission cross section vs incident proton kinetic energy for protons on U^{238}. The experimental data are taken from o Ref. 16, □ Ref. 17, x Ref. 18, ◇ Ref. 19, ▲ Ref. 20, ▼ Ref. 21, and ■ Ref. 22.

Results and Discussion

In Fig. 1. The calculated nonelastic cross section and the calculated fission cross section for protons on U^{238} are shown as a function of incident proton kinetic energy. The points on the calculated curves indicate the energies at which calculations have actually been carried out. The dashed and solid curves are drawn through the calculated points to aid in interpreting the figure. The error bars on the calculated points are statistical only and represent one standard deviation. The fission cross section values shown in the figure were calculated with B_0 = 11 MeV (see Eq. 25), but these results are quite insensitive to the value used. The calculated results shown in Fig. 1 are not appreciably different from the results obtained earlier by Hahn and Bertini.

Also shown in Fig. 1 are a large variety of experimentally measured values of the fission cross section for protons of various energies on U^{238}. In the figure only representative results are shown from some of the references because of the large number of points available.

Because of the spread in the experimental fission cross section data it is difficult to say precisely

that the calculated results agree with the experimental data, but it is clear that above about 100 MeV the calculated and experimental fission cross sections are in approximate agreement. The decrease in the fission cross section above approximately 500 MeV where the nonelastic cross section is increasing slightly may be due to the fact that pion production is becoming significant. As the incident proton energy decreases below 100 MeV the calculated fission cross section increases slightly while the very few experimental points do not show the slight increase. This may indicate, as one might expect, that the model becomes inaccurate at the lower energies but more information is needed before this can be said with any certainty.

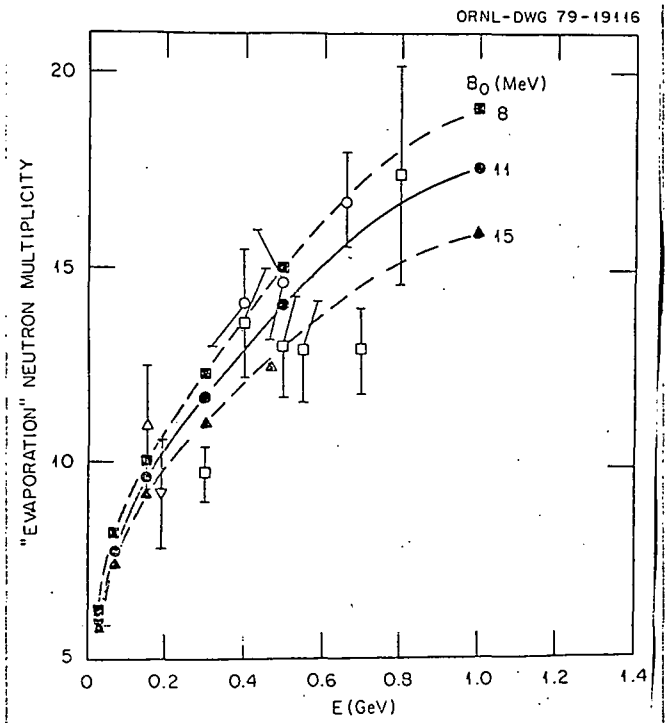

Fig. 2. "Evaporation" neutron multiplicity vs incident proton energy for protons on U^{238}. The experimental data are taken from ▲ Ref. 23, ▽ Ref. 24, □ Ref. 25, and o Ref. 26.

In Fig. 2 the calculated "evaporation" neutron multiplicity is shown as a function of incident energy for protons incident on U^{238}. The designation "evaporation" neutron multiplicity means all neutrons that are obtained from excited "compound" nuclei, and explicitly excludes all neutrons that are emitted during the "cascade" that takes place before a "compound" nucleus is formed. The evaporation neutron multiplicity includes those evaporation neutrons that are emitted before fission takes place, and those evaporation neutrons from the excited nuclei produced by the fission process. The evaporation neutrons have a spectrum that extends into the 25 MeV range, but the large majority are below energies of the order of 10 to 15 MeV.

Also shown in Fig. 2 are a variety of experimental "evaporation" neutron multiplicities for protons on U^{238} taken from Refs. 23-26. These experimentally measured "evaporation" neutron multiplicities are defined only very approximately in the various references and the measured points in Fig. 2 correspond only approximately to the calculated quantities.

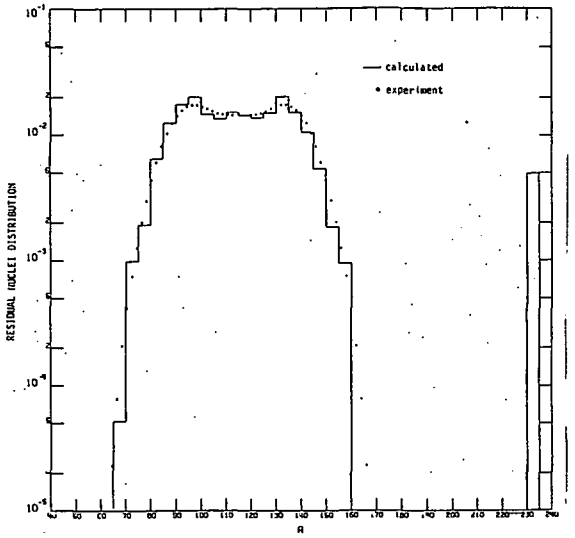

Fig. 3. Residual nuclei distribution from 30 MeV protons on U^{235}. The experimental data for A > 118 is from Ref. 7 and for A < 118 was obtained assuming symmetry as described in the text.

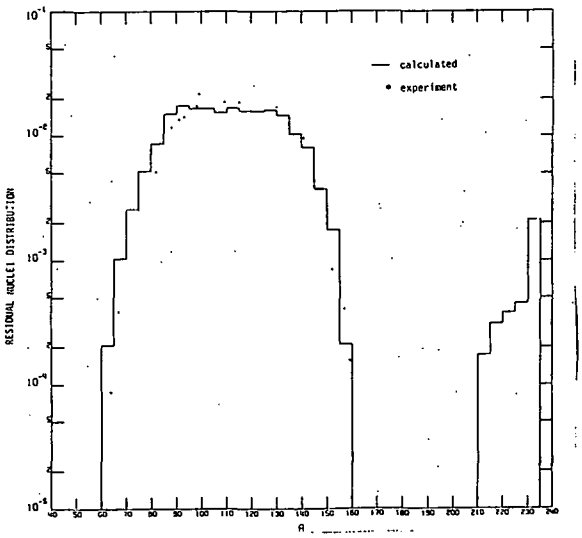

Fig. 4. Residual nuclei distribution from 300 MeV protons on U^{238}. The experimental data are from Ref. 16.

Calculated results are shown in Fig. 2 for three values of the parameter B_0 that occur in the level density formula (see Eq. (25)). As the figure indicates, at the lower energies the calculated evaporation neutron multiplicity is not sensitive to the value of B_0 used, but at an incident energy of 1 GeV the difference in the multiplicity values for the various B_0 values is appreciable. Considering the large spread in data, it is difficult to decide on "best" value of B_0, but from Fig. 2 it seems that B_0 = 11 MeV is a reasonable value. It should be noted, however, that B_0 enters into the present calculations in a variety of complex ways, and therefore it should not be concluded that this value is necessarily appropriate in any other context.

In Fig. 3 the calculated distribution of residual nuclei is shown for the case of 30 MeV protons incident on U^{235} and in Fig. 4 the calculated distribution is shown for the case of 300 MeV protons incident on U^{238}.

In both figures the calculated results are normalized to unity for A < 160.

The experimental data in Fig. 3 for A > 118 is taken from Ref. 7. Error bars on the measurements were not given in Ref. 7 and therefore are not shown. In Ref. 7 measured values were not given for A values less than 118 so the data points in Fig. 3 were obtained by assuming symmetry about a midpoint defined by 1/2 [236 - average neutron multiplicity]. The experimental data in Fig. 4 was taken from Ref. 13 and again experimental error bars are not shown because they were not given in Ref. 9. The normalization on the experimental data is the same as that used (see above) for the calculated data.

The calculated results in Fig. 3 are in very good agreement with the experimental data over the complete range of A values considered. To some extent, this is to be expected because the experimental data was used in obtaining the functions used in the statistical model, but nevertheless, the good agreement shown in Fig. 3 is very satisfying. The calculated results in Fig. 4 are in good agreement with the experimental data at the larger A values ($A \gtrsim 118$) but overestimate the experimental data somewhat for the lower A values. In both Fig. 3 and 4 the residual nuclei for the larger A values ($A \gtrsim 200$) correspond to incident particle collisions in which no fission occurred. No experimental comparisons between calculated results and experimental data for these higher A residual nuclei are considered here but such comparisons are given in Ref. 5.

Acknowledgement

Research sponsored by the U.S. Department of Energy, Office of Basic Energy Sciences, under contract no. W-7405-eng-26 with Union Carbide Corporation.

References

1. Proceedings of an Information Meeting on Accelerator Breeding, Brookhaven National Laboratory, June 18-19, 1977, NTIS CONF-770107.

2. J. M. Carpenter, Nucl. Instr. Methods 145 133 (1977).

3. H. W. Bertini, Phys. Rev. C 6, 631 (1972).

4. H. W. Bertini, "Spallations Reactions: Calculations" in Spallation Nuclear Reactions and Their Applications (D. Reidel Publishing Co., Boston, MA, 1976).

5. R. L. Hahn and H. W. Bertini, Phys. Rev. C 6 660 (1972).

6. P. Fong, Statistical Theory of Nuclear Fission (Gordon and Breach Science Publishers, New York, NY, 1969).

7. D. H. Epperson, "Systematics of Mass Yield Distributions for Nuclear Fission of Neptunium" Dissertation, Dept. of Physics, Duke University, 1978.

8. V. S. Barashenkov and V. D. Toneyev, "Interactions of High-Energy Particles and Atomic Nuclei with Nuclei," Chapter 10, FTD-ID(RS)T-1069-77 (1977).

9. A Michaudon, Proceedings of the International Conference on the Interactions of Neutrons with Nuclei, Lowell, MA, July 6-9, 1976, NTIS CONF-760715-P1.

10. P. Fong, Phys. Rev. Letters 11, (1963).

11. P. Fong, private communication (1978).

12. J. Wing and P. Fong, Phys. Rev. 13C (1964).

13. A. M. Wapstra, Physica 21, 367 (1955).

14. A. G. W. Cameron, Can. J. of Phys. 36, 1040 (1958).

15. K. J. LeCouteur and D. W. Lang, Nucl. Phys. 13, 36 (1959).

16. P. C. Stevenson et al., Phys. Rev. 111, 886 (1958).

17. H. Steiner and H. Jungerman, Phys. Rev. 101, 807 (1956).

18. A. Kjelberg and A. Pappas, Nucl. Phys. 1, 322 (1956).

19. J. Hudis and S. Katcoff, Phys. Rev. 180 1122 (1969).

20. See Ref. 56, p. 352 of Ref. 8.

21. See Ref. 101, p. 352 of Ref. 8.

22. E. S. Matusevich and V. I. Regushevskii, Yadern. Fiz. 7, 1187 (1968) [Transl: Soviet Journal Nucl. Phys. 7, 708 (1968)].

23. E. Cheifetz et al., Phys. Rev. C 2, 256 (1970).

24. E. E. Gross, University of California Report Nos. UCRL-3330 and UCRL-3336 (1956), unpublished.

25. M. Bercovitch et al., Phys. Rev. 119, 412 (1960).

26. R. V. Vasil'kov et al., Yadern. Fiz. 7, 88 (1968) [Transl: Soviet Journal Nucl. Phys. 7, 64 (1968)].